

Theoretical investigation of how edge states are destroyed in disordered mesoscopic samples

Zhenhua Qiao,¹ Jian Wang,^{1,*} Qingfeng Sun,² and Hong Guo³

¹*Department of Physics and The Center of Theoretical and Computational Physics, The University of Hong Kong, Pokfulam Road, Hong Kong, China*

²*Institute of Physics, Chinese Academy of Sciences, Beijing, People's Republic of China*

³*Department of Physics, McGill University, Montreal, Quebec, Canada H3A 2T8*

(Received 1 April 2009; published 7 May 2009)

We report theoretical investigations on how edge states are destroyed in disordered mesoscopic samples by calculating a “phase diagram” in terms of energy versus disorder strength (E, W), and magnetic field versus disorder strength (B, W), in the integer quantum Hall regime. It is found that as the disorder strength W increases, edge states are destroyed one by one if transmission eigenchannels are used to characterize the edge states. Near the insulating regime, transmission eigenchannels are closed one by one in the same order as edge states are destroyed. To identify those edge states which have survived disorder, we introduce a generalized current density that can be calculated and visualized.

DOI: [10.1103/PhysRevB.79.205308](https://doi.org/10.1103/PhysRevB.79.205308)

PACS number(s): 73.23.-b, 72.10.Bg, 73.63.-b

I. INTRODUCTION

When a two-dimensional *mesoscopic* sample is subjected to external magnetic field, peculiar electronic states—edge states, may be established at the boundaries of the sample.^{1,2} Classically, Lorentz force pushes electrons toward the sample boundary and electron trajectories become skipping orbits. Edge states can be considered as the quantum version of skipping orbits.² Importantly, edge states in mesoscopic samples provide necessary density of states (DOS) between the Landau levels, integer quantum Hall effect (IQHE) can therefore occur in the clean sample limit.² In contrast, for infinitely large samples, a degree of disorder in the sample appears necessary which provides DOS in between Landau levels to stabilize the Fermi energy for IQHE.³ Nevertheless, increasing disorder will eventually destroy IQHE and how does this happen has been an important issue attracting numerous studies.

Here we address the disorder issue for *mesoscopic* samples, namely, how edge states are destroyed by disorder in the IQHE regime and, at a fixed filling factor $\nu > 1$, are edge states destroyed all at once or one by one. These important questions provide insight to the IQHE phase diagram for mesoscopic samples, and may shed light to similar problems in samples of infinite size. We address these questions by extensive calculations on a mesoscopic graphene system⁴ and a square lattice model [see inset of Fig. 1(a)] to map out a “phase diagram” of edge states in the presence of disorder. Here the “phases” in the “phase diagram” denote quantum states and no phase transitions are implied between these states. We use transmission eigenchannels to characterize edge states (see below), and we found that they are destroyed one by one. At large enough disorder, the system becomes an insulator and transmission eigenchannels are closed one by one in the same order as the edge states are destroyed.

We begin by discussing our definition of edge states as well as the way to visualize them. In transport theory, for each incoming channel of a semi-infinite lead α whose wave function is $|W_{\alpha,m}\rangle$ where $m=1, 2, \dots, N$ denotes one of the N channels, one solves a scattering problem. $|W_{\alpha,m}\rangle$ is an eigenchannel of lead α but not the entire device. To find the eigen-

channels of the entire device, we diagonalize⁵ the transmission matrix T by a unitary transformation U , for a two-probe device having scattering matrix S_{RL} , $T=S_{RL}^\dagger S_{RL}$. Mathematically, this means acting U on the incoming channels $|W_{\alpha,m}\rangle$ (which is a column vector with N components) to obtain a new set of orthogonal incoming modes $|\bar{W}_{\alpha,m}\rangle = \sum_n |W_{\alpha,n}\rangle U_{nm}$. Once done, $|\bar{W}_{\alpha,m}\rangle$ is an *eigenstate* of the entire device (leads plus scattering region). In other words, if an incoming electron comes at state $|\bar{W}_{\alpha,m}\rangle$, it will traverse the entire device without mixing with any other eigenstate $|\bar{W}_{\alpha,m'}\rangle$. This way, the resulting transmission matrix $\bar{T} = U^\dagger T U$ is diagonal. In the presence of a strong magnetic field B , it is therefore natural to identify $|\bar{W}_{\alpha,m}(B)\rangle$ as edge states because they are the eigenstates or eigenchannels of the entire device sample. How to visualize edge states in the IQHE regime? This may be achieved by plotting the current

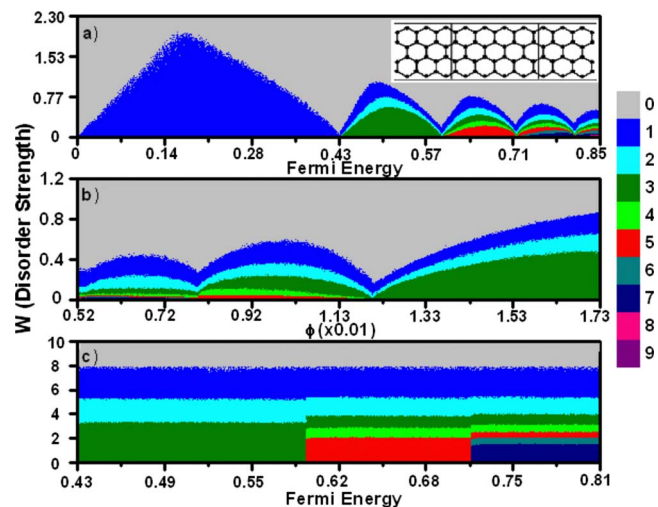


FIG. 1. (Color online) (a) and (b) are “phase diagram” of edge states of a zigzag graphene ribbon for energies near the Fermi level (Dirac electrons): (a) in the (E, W) plane; (b) in the (B, W) plane. (c) The order of closing of eigenchannels at large disorder. Color coding is for number of eigenchannels.

density in real space. The subtle issues of current density in IQHE have been discussed in Ref. 6. In our work where there are disorders in the sample, the eigenchannels provide a convenient way to define a generalized current density for each channel—since the eigenchannels do not mix. Clearly, the total transport current is obtained by integrating current density along any cross section perpendicular to the transport direction.

II. NUMERICAL STUDY

The total transmission coefficient is obtained from the $N \times N$ Hermitian transmission matrix $\mathcal{T}=\{t_{ij}\}$. Applying an unitary transformation U ,⁵ we obtain $\bar{\mathcal{T}}=U^\dagger \mathcal{T} U=\{t_i \delta_{ij}\}$, which is diagonal with elements t_i . The transmission coefficient t_i of eigenchannel i is a linear combination of t_{ij} . Using conventional current density $\mathbf{J}_{ii}=(ie\hbar/2m)(\psi_i \nabla \psi_i^* - \psi_i^* \nabla \psi_i) - (e^2/m)\mathbf{A}|\psi_i|^2$ with $i=1,2,\dots,N$, it is easy to show $(e^2/h)t_{ii}=\int \mathbf{J}_{ii} \cdot d\mathbf{s}$ in the linear bias regime, where t_{ii} is the diagonal element of matrix \mathcal{T} . In order to find an *eigencurrent density* \mathbf{J}_i such that

$$\frac{e^2}{h}t_i = \int \mathbf{J}_i \cdot d\mathbf{s}, \quad (1)$$

we define a generalized complex current density \mathbf{J}_{ij} so that $(e^2/h)t_{ij}=\int \mathbf{J}_{ij} \cdot d\mathbf{s}$. The unitary transformation on the incoming wave function $|W_{\alpha,m}\rangle$ suggests the following definition:

$$\mathbf{J}_{ij} = \frac{ie\hbar}{2m}(\psi_j \nabla \psi_i^* - \psi_i^* \nabla \psi_j) - \frac{e^2}{m}\mathbf{A}\psi_j\psi_i^*, \quad (2)$$

where ψ_i is the wave function in the scattering region due to the incoming state $|W_{\alpha,i}\rangle$. From this definition, we can prove the relationship $(e^2/h)t_{ij}=\int \mathbf{J}_{ij} \cdot d\mathbf{s}$, as follows. It is not difficult to show that the following \mathbf{J}_i satisfies Eq. (1):

$$\mathbf{J}_i = (ie\hbar/2m)(\bar{\psi}_i \nabla \bar{\psi}_i^* - \bar{\psi}_i^* \nabla \bar{\psi}_i) - (e^2/m)\mathbf{A}|\bar{\psi}_i|^2, \quad (3)$$

where $\bar{\psi}_i=\sum_j \psi_j U_{ji}$. Using this \mathbf{J}_i , Eq. (1) becomes

$$\frac{e^2}{h}t_i = \int \sum_{jk} U_{ji} U_{kj}^* \mathbf{J}_{kj} \cdot d\mathbf{s}. \quad (4)$$

Denoting \mathcal{J}_G the generalized current-density matrix with matrix elements \mathbf{J}_{ij} , Eq. (4) is equivalent to

$$\frac{e^2}{h}\bar{\mathcal{T}}=U^\dagger \int \mathcal{J}_G \cdot d\mathbf{s} U \quad \text{or} \quad \frac{e^2}{h}\mathcal{T}=\int \mathcal{J}_G \cdot d\mathbf{s}. \quad (5)$$

We have also confirmed Eq. (3) numerically using specific examples including that shown in the inset of Fig. 1(a). Therefore, to obtain eigen-current-density matrix, we first diagonalize the transmission matrix \mathcal{T} to find the unitary matrix U ; we then calculate the generalized current density \mathcal{J}_G according to Eq. (2). The eigen-current-density matrix is finally obtained by $\mathcal{J}_{\text{eigen}}=U^\dagger \mathcal{J}_G U$ and plotted for visualization.

Can eigenchannels be measured experimentally? To answer this question, as an example let us consider a two-probe device having two eigenchannels or two edge states in the presence of magnetic field. Assume one can perform two

experiments: (i) measurement of conductance and (ii) measurement of shot noise. Clearly, conductance is given by

$$G = \frac{e^2}{h}(t_1 + t_2). \quad (6)$$

The shot noise is given by⁵

$$S = \frac{e^2}{h}[t_1(1-t_1) + t_2(1-t_2)]. \quad (7)$$

From these t_1 and t_2 can be determined. In the case of three eigenchannels, one needs to experimentally measure an additional quantity,⁷ for instance the third cumulant of current,

$$Y = \langle \Delta \hat{I}(t_1) \Delta \hat{I}(t_2) \Delta \hat{I}(t_3) \rangle. \quad (8)$$

In the linear regime, $Y=(e^2/h)\sum_i t_i(1-t_i)(1-2t_i)$.⁸ Hence by measuring G , S , and Y , one can determine $t_{1,2,3}$. Therefore, the transmission eigenchannels are physical quantities measurable experimentally.

Having prepared analytical tools, we now present numerical calculations on how the edge states are destroyed by increasing degrees of disorder. In the tight-binding representation, the Hamiltonian of a 2D graphene sheet can be written as

$$H = \sum_i \epsilon_i c_i^\dagger c_i - t \sum_{\langle ij \rangle} e^{i2\pi\phi_{ij}} c_i^\dagger c_j, \quad (9)$$

where $c_i^\dagger(c_i)$ is the creation (annihilation) operator for an electron on site i . The first term in H is the on-site single-particle energy where diagonal disorder is introduced by drawing ϵ_i randomly from a uniform distribution in the interval $[-W/2, W/2]$ where W measures the disorder strength. In the absence of disorder, the on-site energy is $4t$. The second term in H is due to nearest-neighbor hopping that includes the effect of a magnetic field. Here the phase $\phi_{ij}=\int \mathbf{A} \cdot d\mathbf{l} / \phi_0$ and $\phi_0=h/e$ is the flux quanta. We fix gauge so that $\mathbf{A}=(By, 0, 0)$; and current flows in the x direction. Transmission coefficient is given by $T=\text{Tr}[\mathcal{T}]$ where the transmission matrix \mathcal{T} is obtained from $\mathcal{T}=\Gamma_R G^r \Gamma_L G^a$ with $G^{r,a}$ being the retarded and advanced Green's functions of the disordered scattering region. Quantities Γ_α ($\alpha=L,R$) are the linewidth functions obtained by calculating self-energies Σ^r due to the semi-infinite leads.⁹ The numerical data are mainly obtained from systems with 32×56 sites. In the calculations, energy and disorder strengths are measured in unit of coupling strength t .

In order to use Eqs. (2) and (3) to calculate the current density, we note that the scattering wave-function appeared in Eq. (2) is related to the Green's function,¹⁰

$$|\psi_{\alpha m}\rangle = \kappa_m G^r |W_{\alpha m}\rangle, \quad (10)$$

where $|W_{\alpha m}\rangle$ is the m th renormalized eigenstate of linewidth function matrix Γ_α such that $\Gamma_\alpha=\sum_m |W_{\alpha m}\rangle \langle W_{\alpha m}|$. The channel number m depends on the energy of incident electron, $\kappa_m=\sqrt{\hbar v_m}$, and v_m is the channel group velocity. Substituting Eq. (10) into Eqs. (2) and (3), the generalized current density can be expressed in terms of the Green's functions.

Numerically, an edge state is identified if transmission coefficient of an eigenchannel is $T \geq 0.999$ (Ref. 11); if T

≤ 0.001 , the eigenchannel is said to be closed. In addition, an edge state is said to be “destroyed” by disorder and becomes a regular eigenchannel if its transmission T drops to below 0.999. Figure 1(a) plots the phase diagram of edge states of graphene in the (E, W) plane with $\phi=0.0173$ and energy range $[0, 0.85]$ where band dispersion is linear (Dirac electrons). A mesh of 600×480 points is scanned in (E, W) plane and up to 200 disorder configurations are averaged at each point. Several observations are in order. First, the edge states are destroyed one by one as W is increased. For instance, at $E=0.5$ the $\nu=3$ edge state is destroyed when $W=0.5$. Very importantly, we emphasize that at this disorder, there are still three transmission eigenchannels although only two are edge states and the third being a regular eigenchannel having $T < 0.999$. In other words, the third eigenchannel is still there to participate transport although it is no longer an edge state. Increasing disorder to $W=0.7$, the $\nu=2$ edge state is destroyed; finally when $W=1$, all three edge states are destroyed. We note that edge states would be destroyed all at once if we had used the usual transmission coefficient for each channel t_{ii} to characterize the edge states. Second, upon further increasing W , an insulating state is reached where all eigenchannels are closed. The order of channel closing is also one by one, in the same order as how edge states are destroyed. This is shown in Fig. 1(c). For instance, at $E=0.5$ there are three eigenchannels to start with, and at large disorder $W=3.1$, one of them is closed leaving only two regular eigenchannels. Third, the edge states are easily destroyed at the subband edges while at the subband center they are most robust against disorder. This is true even at the Dirac point with $E=0$. This is because the energy of Landau levels is located at the subband edge. In the presence of disorder, the Landau level is broadened with a finite width.¹ Hence the edge state that is close to one Landau level can easily relax toward it. Fourth, it is more difficult to destroy an edge state at smaller energies. For Dirac electrons, the density of states is proportional to \sqrt{E} so that the level spacing of lower Landau levels is larger than the upper ones. For electrons with smaller energy it is farther away from nearby Landau level than electrons with larger energy. Hence a larger disorder is needed to relax the electrons to the nearby Landau level. Finally, Fig. 1(b) plots a “phase diagram” of edge states in the (B, W) plane for Dirac electrons. Once again, the edge states are destroyed one by one, similar to the phase diagram in the (E, W) plane.

Figure 2(a) depicts the “phase diagram” of edge states of graphene in (E, W) plane for higher energies in the range $E = [2.545, 2.97]$, where holelike behavior occurs and band dispersion is nonlinear (non-Dirac electrons). Again, edge states are destroyed one by one. While the “phase diagram” topology is similar to that for Dirac electrons (Fig. 1), here the band dispersion is quadratic with equal-energy spacing between the Landau levels. Due to this reason, the values of W that are needed to destroy the last edge state at different subband centers are almost the same. We have also calculated the “phase diagram” of edge states of a square lattice in the (E, W) plane using the same numerical method, results are shown in Fig. 2(b) which are rather similar Fig. 2(a). In particular, it is more difficult to destroy edge states at low filling factor ν , consistent with the result of Ref. 12. We have

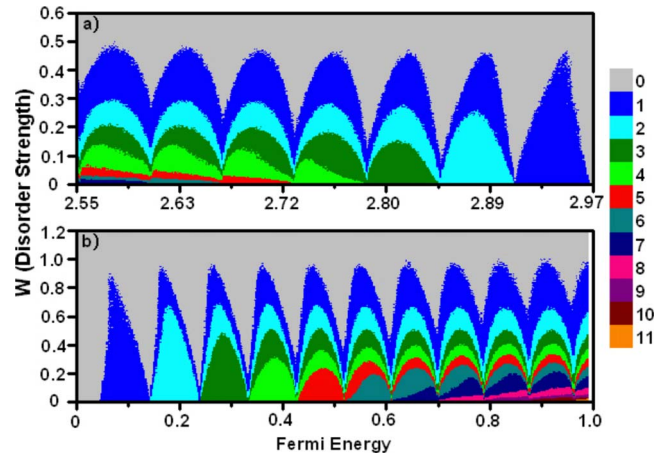


FIG. 2. (Color online) Phase diagram of edge states in (E, W) plane for: (a) holelike charge carriers in the zigzag graphene ribbon; (b) electrons in a square lattice. The main difference between the two phase diagrams is due to opposite charges of hole and electron.

also studied the phase diagram of edge states of an armchair graphene ribbon and found that the behavior is qualitatively the same as that of zigzag graphene ribbons.

Next, we examine the nature of those edge states that have survived disorder by calculating current density from Eqs. (2) and (3) and plotting it along the propagating direction (x direction). Figure 3 shows the current density of two edge states in the absence of disorder for the square lattice model. Edge states are clearly seen. Since the two transmission eigenchannels have different longitudinal energies or effective velocities along the propagating direction, it gives two different skipping patterns that correspond to two different skipping orbits of classical trajectory.¹³ In Fig. 3(a), current flows in the negative direction (blue region) near the sample boundary and in the positive direction (red region) away from it. There is a region between these opposite flows where the current density is very small. The classical trajectory of an electron under Lorentz force is depicted in the

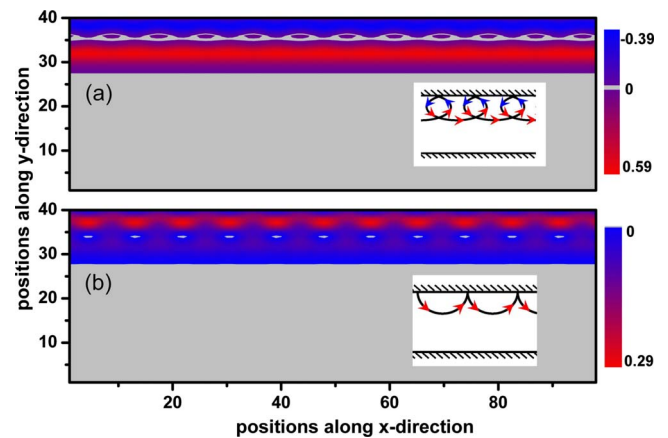


FIG. 3. (Color online) Current density of two edge states flowing from left to right along x direction, for a square lattice of 100×40 sites in the absence of disorder. Here $E=0.4$ and $\phi=0.052$. Note that the color scale is different for the two panels. Insets: classical skipping orbits.

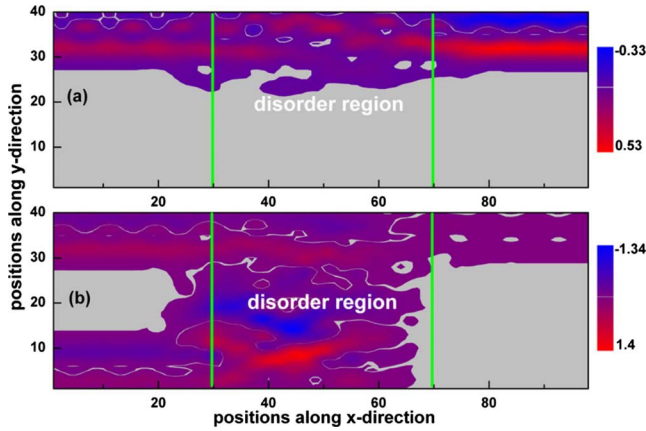


FIG. 4. (Color online) Current density along x direction for the square lattice model as that of Fig. 3, with disorder strength $W=1$, energy $E=0.4$, and magnetic field $\phi=0.052$. (a) For an edge state that has survived disorder; (b) edge state that has been destroyed by disorder.

inset, showing a nearly completed circular motion before colliding with the sample boundary. There is a one-to-one correspondence between the classical and quantum motions: near the sample boundary the flow is from right to left, while it flows opposite away from the boundary. Similar one-to-one correspondence is also seen in Fig. 3(b). For the same square lattice model, Figs. 4 and 5 plot the x and y components of current density of two eigenchannels for a particular disorder configuration $W=1$ where the eigentransmission coefficients are $T_1=0.9999$ and $T_2=0.3385$, respectively. In the numerical calculation, we have confirmed that the integral of \mathbf{J}_i over any cross-section area along the propagating direction gives the same value that is equal to $(e^2/h)t_i$. From Figs. 4(a) and 5(a), it is obvious that $T_1=0.9999$ is an edge state that survived this degree of disorder. Compare to Fig. 3, the pattern of current density with disorder scattering is clearly different. For the eigenchannel with $T_2=0.3385$, it is clearly a nonedge state [Fig. 4(b)]: there is a circulating pattern with

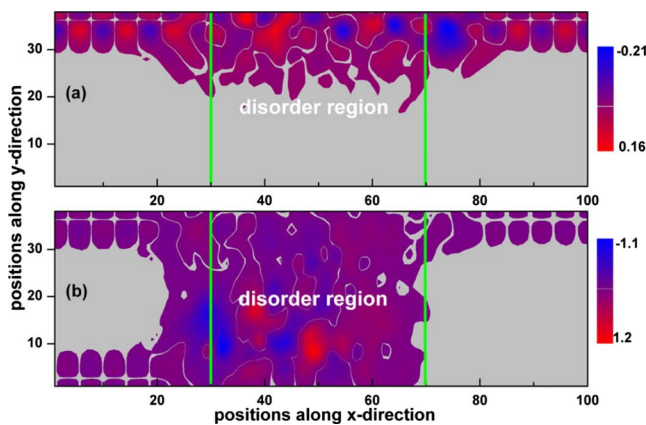


FIG. 5. (Color online) Current density along y direction for the square lattice model as that of Fig. 3, with disorder strength $W=1$, energy $E=0.4$, and magnetic field $\phi=0.052$. (a) For an edge state that has survived disorder; (b) edge state that has been destroyed by disorder.

large current density in the middle of the scattering region, caused by the disorder scattering. Finally, we have also calculated current density for edge states in disordered graphene ribbons, and similar behaviors are observed as that of Fig. 4.

III. SUMMARY AND DISCUSSION

In summary, we have investigated the nature of edge states in disordered mesoscopic samples in the IQHE regime. Our results show that edge states are destroyed one by one as disorder strength is increased. In the insulating regime, all transmission eigenchannels are closed and the closing is also one by one in the same order as the edge states were destroyed. For graphene and the square lattice model, the “phase diagrams” have similar topology but with some differences due to band dispersions. We have introduced a quantity which is the generalized current density, using it the current density of each eigenchannel can be calculated in the presence of disorder, giving us a vivid physical picture on how edge states are destroyed. Since transmission coefficients of individual eigenchannels for mesoscopic samples can be determined experimentally in the IQHE regime—as we discussed in the paper, our conclusions on how edge states are destroyed by disorder should be testable experimentally.

We note in passing that how to generalize our results to the large sample limit is an interesting problem requiring further investigation. In particular, based on the picture of Khmel'nitskii¹⁴ and Laughlin,¹⁵ a global phase diagram of quantum Hall effect in the (B, W) plane was proposed by Kivelson *et al.*¹⁶ for large samples which attracted considerable attention both theoretically^{12,17} and experimentally.¹⁸ According to it, an integer quantum Hall state with a fixed filling factor ν will *float up* in energy as the disorder strength increases.^{14,15} In the context of *mesoscopic* sample, this idea would mean the following. Consider Fermi level $E=E_f$ at the mesoscopic sample boundary there are, say, ν edge states whose eigenvalues cut this energy E_f . The “float up” idea means that when disorder is increased, the energies of edge states increase to higher values, i.e., they float up. Hence, at large enough disorder there will only be $\nu-1$ edge states cutting E_f . This way, the system undergoes a series of transitions between ν to $\nu-1$ states etc. Our results presented above, however, indicate that for mesoscopic samples edge states do not float up by disorder, they are destroyed to become regular transmission eigenchannels which participate transport.

ACKNOWLEDGMENTS

We thank Y.X. Xing for helpful discussions on the classical analogy of edge states. H.G. wishes to thank X.C. Xie and Q. Niu for useful discussions on global phase diagram of quantum Hall effect. J.W. is financially supported by a RGC grant (Grant No. HKU 704607P) from HKSAR and LuXin Energy Group. Q.F.S. is supported by NSF-China under Grants No. 10525418 and No. 10734110; H.G. by NSERC of Canada, FQRNT of Québec and CIFAR.

*jianwang@hkusua.hku.hk

- ¹B. I. Halperin, Phys. Rev. B **25**, 2185 (1982).
²M. Büttiker, Phys. Rev. B **38**, 9375 (1988).
³R. E. Prange, in *The Quantum Hall Effect* (Springer-Verlag, New York, 1987).
⁴K. S. Novoselov *et al.*, Nature (London) **438**, 197 (2005); Y. Zhang *et al.*, *ibid.* **438**, 201 (2005).
⁵M. Büttiker, Phys. Rev. B **46**, 12485 (1992).
⁶S. Komiyama and H. Hirai, Phys. Rev. B **54**, 2067 (1996).
⁷B. Reulet, J. Senzier, and D. E. Prober, Phys. Rev. Lett. **91**, 196601 (2003).
⁸M. Kindermann, Yu. V. Nazarov, and C. W. J. Beenakker, Phys. Rev. Lett. **90**, 246805 (2003).
⁹M. P. López Sancho, J. M. López Sancho, and J. Rubio, J. Phys. F: Met. Phys. **14**, 1205 (1984).
¹⁰J. Wang and H. Guo, Phys. Rev. B **79**, 045119 (2009).
¹¹Although this definition seems to be somewhat arbitrary, one could also use, for example, $T=0.9$ as the definition of edge states. However our calculation shows that the qualitative feature of phase diagram does not depend on the definition of edge states.
¹²D. N. Sheng and Z. Y. Weng, Phys. Rev. Lett. **78**, 318 (1997).
¹³C. W. J. Beenakker and H. van Houten, Solid State Phys. **44**, 1 (1991).
¹⁴D. E. Khmel'nitskii, Phys. Lett. **106A**, 182 (1984).
¹⁵R. B. Laughlin, Phys. Rev. Lett. **52**, 2304 (1984).
¹⁶S. Kivelson, D. H. Lee, and S. C. Zhang, Phys. Rev. B **46**, 2223 (1992).
¹⁷D. Z. Liu, X. C. Xie, and Q. Niu, Phys. Rev. Lett. **76**, 975 (1996); T. Koschny, H. Potempa, and L. Schweitzer, *ibid.* **86**, 3863 (2001); H. Song, I. Maruyama, and Y. Hatsugai, Phys. Rev. B **76**, 132202 (2007).
¹⁸I. Glazman, C. E. Johnson, and H. W. Jiang, Phys. Rev. Lett. **74**, 594 (1995); T. Okamoto, Y. Shinohara, and S. Kawaji, Phys. Rev. B **52**, 11109 (1995); S. V. Kravchenko, W. Mason, J. E. Furneaux, and V. M. Pudalov, Phys. Rev. Lett. **75**, 910 (1995); S. H. Song, D. Shahar, D. C. Tsui, Y. H. Xie, and D. Monroe, *ibid.* **78**, 2200 (1997); C. H. Lee, Y. H. Chang, Y. W. Suen, and H. H. Lin, Phys. Rev. B **58**, 10629 (1998); M. Hilke, D. Shahar, S. H. Song, D. C. Tsui, and Y. H. Xie, *ibid.* **62**, 6940 (2000).